UDC 681.7:520
DOI: 10.20535/2077-7264.1(75).2022.265685

© O. V. Dubolazov, Doctor of physics and mathematics of science, Associate professor, I. V. Soltys, PhD in physics and mathematics science, Associate professor, M. P. Horskyi, PhD in physics and mathematics science, Associate professor, M. M. Matymish, student, Chernivtsi National University, Chernivtsi, Ukraine

MULTILEVEL DIGITAL ALGORITHMS FOR STATISTICAL ANALYSIS OF MICROSCOPIC IMAGES FOR DIFFERENTIATING TEMPERATURE CHANGES IN POLYGRAPHIC POLYMERS

This work is aimed at generalizing the methods of laser polarimetry to the case of partially depolarizing optically anisotropic polymer layers. Mueller's differential matrix mapping method was proposed and substantiated for reproducing the distributions of the parameters of linear and circular birefringence and dichroism of methyl acrylate layers under different temperature conditions (200 — group 1) and (450 — group 2).

Keywords: polarization; optical anisotropy; methyl acrylates; temperature control.

Introduction

Among most methods for polarization studies of phase-inhomogeneous layers of different origin, analytical approaches, which are based on the optical-thin-layer approximation, predominate. This approximation assumes a predominantly single scattering of laser radiation in the volume of the phase-inhomogeneous layer. In such a situation, there is an unambiguous diagnostic relationship between the polarization parameters of the object field and the optical anisotropy maps. However, this approximation is very rarely realized in real diagnostic practice using polarized laser radiation.

Most polymer objects are partially depolarizing. Therefore, it is urgent to further develop and generalize the methods of MMP of the polycrystalline structure of polymer layers with different light scattering multiplicity, or different depolarizing ability [1–5].

This work is aimed at investigating the possibilities of differentiating changes in the optical anisotropy of methyl acrylate layers from group 1 and group 2.

Methods

The optical measurement scheme is shown in fig. 1 [6–8].

Samples 6 were irradiated with a parallel ($\varnothing = 2 \cdot 10^3 \mu m$) low-intensity (W = 5,0 mW) beam of a He-Ne laser (λ = 0,6328). The polarizing feed consists of 3 quarter-wave plates, (Achromatic True Zero-Order Waveplate) and 4 polarizer (B+W Kaesemann XS-Pro Polarizer MRC Nano).

Polymer layer *6* was sequentially probed with a laser beam with the following types of polarization: linear with azimuths of 0°, 90°, +45° and right circulation ($\otimes$).

Polarized images of the polymer layer using polarizing microlens 7 (Nikon CFI Achromat P, focal length — 30 mm, numerical aperture — 0,1, magnification — 4x) were projected into the plane of the photosensitive area (mxn = 1280x960 pixels) of the CCD camera 10 (The Imaging Source DMK 41AU02.AS, monochrome 1/2 "CCD, Sony ICX205AL (progressive scan) resolution — 1280x960, size of the photosensitive area — 7600x6200 μm; sensitivity — 0,05 lx; dynamic range — 8 bit, SNR — 9 bit).

Image analysis of polymer layers *6* was carried out using a polarizer *9* and a quarter-wave plate *8*.

The calculations within each pixel of the digital camera 10 of the set of elements of the Mueller matrix M_{ik} of the sample of the polymer layer were carried out in accordance with the algorithm [9, 10]

$$
\begin{aligned}
&M_{11} = 0.5(V_1^0 + V_1^{90});\\
&M_{12} = 0.5(V_1^0 - V_1^{90});\\
&M_{13} = V_1^{45} - M_{11};\\
&M_{14} = V_1^{\otimes} - M_{11};\\
\\
&M_{21} = 0.5(V_2^0 + V_2^{90});\\
&M_{22} = 0.5(V_2^0 - V_2^{90});\\
&M_{23} = V_2^{45} - M_{21};\\
&M_{24} = V_2^{\otimes} - M_{21};\\
\\
&M_{31} = 0.5(V_3^0 + V_3^{90});\\
&M_{32} = 0.5(V_3^0 - V_3^{90});\\
&M_{33} = V_3^{45} - M_{31};\\
&M_{34} = V_3^{\otimes} - M_{31};\\
\\
&M_{41} = 0.5(V_4^0 + V_4^{90});\\
&M_{42} = 0.5(V_4^0 - V_4^{90});\\
&M_{43} = V_4^{45} - M_{41};\\
&M_{44} = V_4^{\otimes} - M_{41}.
\end{aligned}
\tag{1}
$$

Here $V_{i=2;3;4}^{0;45;90;\otimes}$ — parameters of the Stokes vector of points of a

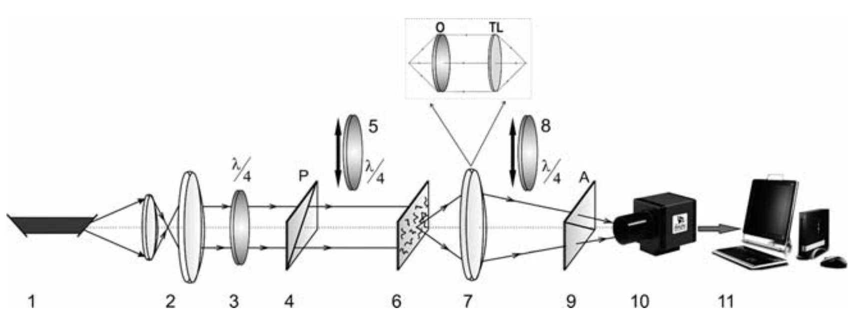

Fig 1. Optical scheme of the polarimeter, where 1 — He-Ne laser; 2 — collimator; 3 — stationary quarter-wave plate; 5, 8 — mechanically movable quarter-wave plates; 4, 9 — polarizer and analyzer; 6 — polymer layer; 7 — polarizing microlens; 10 — CCD camera; 11 — personal computer

ISSN 2077-7264. Технологія і техніка друкарства. 2022. № 1(75)

ISSN 2077-7264. Технологія і техніка друкарства. 2022. № 1(75)

digital image of a polymer layer sample measured for a series of linearly (0^0; 45^0; 90^0) and right-circularly (⊗) polarized laser beams

$$\begin{aligned} V_{i=1}^{0;45;90;\otimes} &= I_{0}^{0;45;90;\otimes} + I_{90}^{0;45;90;\otimes}; \\ V_{i=2}^{0;45;90;\otimes} &= I_{0}^{0;45;90;\otimes} - I_{90}^{0;45;90;\otimes}; \\ V_{i=3}^{0;45;90;\otimes} &= I_{45}^{0;45;90;\otimes} - I_{135}^{0;45;90;\otimes}; \\ V_{i=4}^{0;45;90;\otimes} &= I_{\otimes}^{0;45;90;\otimes} + I_{\oplus}^{0;45;90;\otimes}. \end{aligned} \quad (2)$$

Here $I_{0;45;90;135;\otimes;\oplus}$ — the intensity of the light transmitted by the object, passed through the linear polarizer 9 with the angle Θ of rotation of the transmission plane: 0^0; 45^0; 90^0; 135^0, as well as through the «quarter-wave plate—polarizer» system of the polarization analysis block, which transmits the right- (⊗) and left- (⊕) circularly polarized components of the object laser radiation.

Expression for calculating the elements of a differential matrix of the 1st order [3, 4].

$$\langle\{m\}\rangle = \\ = z^{-1}\left\| \begin{matrix} 0 & \ln\left(0.25(V_1^0-V_1^{90})(V_2^0+V_2^{90})\right) & 0.5\ln\left(V_1^{45}-M_{11})(V_3^0+V_3^{90})\right) & 0.5\ln\left(\left(V_1^{\otimes}-M_{11}\right)(V_4^0+V_4^{90})\right) \\ \ln\left(0.5(V_1^0-V_1^{90})0.5(V_2^0+V_2^{90})\right) & 0 & \ln\left(\frac{V_2^{45}-M_{21}}{0.5(V_3^0-V_3^{90})}\right) & \ln\left(\frac{V_2^{45}-M_{21}}{0.5(V_4^0-V_4^{90})}\right) \\ 0.5\ln\left(V_1^{45}-M_{11})(V_3^0+V_3^{90})\right) & \ln\left(\frac{0.5(V_3^0-V_3^{90})}{V_2^{45}-M_{21}}\right) & 0 & \ln\left(\frac{V_3^{\otimes}-M_{31}}{V_4^{45}-M_{41}}\right) \\ \ln\left(M_{14}M_{41}\right) & \ln\left(\frac{0.5(V_4^0-V_4^{90})}{V_2^{45}-M_{21}}\right) & \ln\left(\frac{V_4^{45}-M_{41}}{V_3^{\otimes}-M_{31}}\right) & 0 \end{matrix} \right\|. \quad (3)$$

Results

The results of studying the capabilities of the method of differential Mueller-matrix mapping of the completely polarized polycrystalline component of optically thick (attenuation coefficient $\tau = 0,83 \div 0,91$) layers of methyl acrylate from group 1 (31 samples) and group 2 (31 samples) are presented.

In fig. 2 and fig. 3 shows a series of histograms of the distributions of the averaged parameters of linear and circular birefringence (LB; CB; LB' — fig. 2) and dichroism (LD; CD; LD' — fig. 3) of methyl acrylate layers from group 1 (fig. 2, fig. 3, fragments (1)–(3)) and group 2 (fig. 2, fig. 3, fragments (4)–(6)).

Discusion

The quantitative transformations of the polycrystalline structure of optically thick layers of methyl acrylate are illustrated by the data of the statistical analysis of two-dimensional distributions of the magnitude of the elements

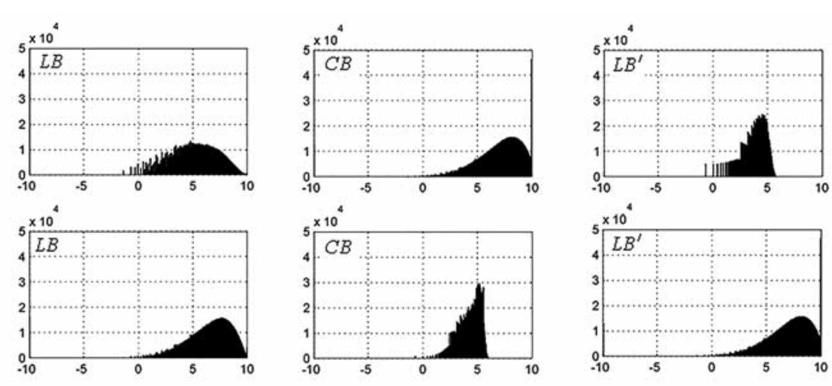

Fig. 2. Histograms of the distribution of the linear (fragments (1), (3), (4)) and circular (fragments (2), (5)) birefringence of methyl acrylate layers from group 1 (fragments (1)–(3)) and group 2 (fragments (4)–(6))

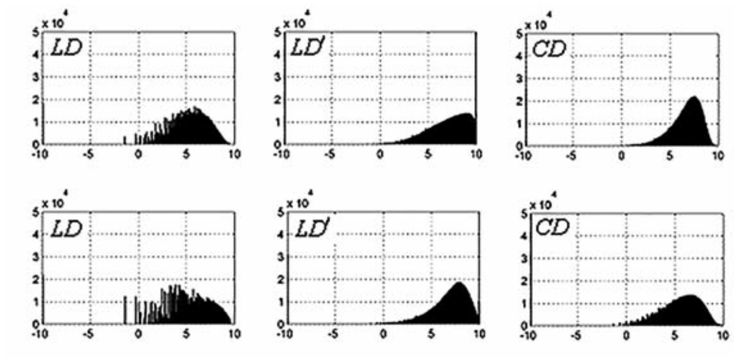

Fig. 3. Histograms of the distribution of the linear (fragments (1), (3), (4)) and circular (fragments (2), (5)) dichroism of methyl acrylate layers from group 1 (fragments (1)–(3)) and group 2 (fragments (4)–(6))

of the first-order differential matrix of the fully polarized component of the depolarizing polycrystalline networks.

Table 1 and Table 2 show the average values and average errors of the statistical ($Z_{i=1;2;3;4}$) parameters characterizing the distributions of the values $\langle\{m_{ik}\}\rangle$ of the methyl acrylate layers of both groups.

Comparative analysis of the aggregate of statistical moments of the 1st–4th orders revealed the following ones that are most sensitive to changes in the phase and amplitude anisotropy of methyl acrylate layers from group 1 and group 2 against the background of a depolarized background of multiply scattered radiation (highlighted in gray):

$$\begin{cases} \Delta Z_3\left(LB, CB, LB'\right) = \\ = 2,42 \div 2,83 - (Ac = 91\%); \\ \Delta Z_4\left(LB, CB, LB'\right) = \\ = 2,15 \div 5,97 - (Ac = 94\%); \end{cases}$$

Table1

Statistical moments of the 1st–4th orders characterizing the distributions LB; CB; LB' of methyl acrylate layers from group 1 and group 2

Z_i	$\langle\{m_{23;32}\}\rangle$		$\langle\{m_{24;42}\}\rangle$		$\langle\{m_{34;43}\}\rangle$	
Z_1	5,75±0,33	8,16±0,57	3,27±0,16	7,09±0,47	3,57±0,19	7,34±0,49
Z_2	4,23±0,28	2,87±0,16	1,93±0,12	3,41±0,18	1,84±0,11	3,67±0,21
Z_3	0,62±0,036	1,69±0,11	2,12±0,13	0,87±0,052	1,92±0,14	0,73±0,044
Z_4	0,41±0,028	0,88±0,054	1,96±0,13	0,41±0,025	1,71±0,09	0,34±0,019

ISSN 2077-7264. Технологія і техніка друкарства. 2022. № 1(75)

Table 2

Statistical moments of the 1st–4th orders characterizing the distributions LD; CD: LD’ of methyl acrylate layers from group 1 and group 2

Z_i	$\langle\{m_{12;21}\}\rangle$		$\langle\{m_{13;31}\}\rangle$		$\langle\{m_{14;41}\}\rangle$	
Z_1	4,12±0,26	5,29±0,33	7,86±0,45	6,13±0,39	6,21±0,41	5,85±0,37
Z_2	6,22±0,39	4,74±0,27	4,15±0,23	3,36±0,18	3,41±0,19	2,72±0,15
Z_3	0,85±0,051	0,66±0,038	1,96±0,12	0,87±0,052	1,14±0,058	0,74±0,043
Z_4	0,74±0,044	0,43±0,027	0,82±0,053	0,51±0,031	0,72±0,044	0,44±0,029

Conclusions

1. A method of differential Muller-matrix mapping is proposed and substantiated for reproducing the distributions of the parameters of linear and circular birefringence and dichroism of partially depolarizing methyl acrylate layers from group 1 and group 2.

2. Achieved good ($\Delta Z_{3;4}(LD, CD, LD') \Rightarrow Ac \succ 80\,\%$) and excellent ($\Delta Z_{3;4}(LB, CB, LB') \Rightarrow Ac \succ 90\,\%$) diagnostic quality by the method of differential Mueller-matrix mapping of partially depolarizing methyl acrylate layers from group 1 and group 2.

References

1. Ushenko, Y. A., Boychuk, T. M., Bachynsky, V. T., & Mincer, O. P. (2013). Diagnostics of Structure and Physiological State of Birefringent Biological Tissues: Statistical, Correlation and Topological Approaches. Handbook of Coherent-Domain Optical Methods. New York: Springer Science+Business Media, 107.
2. Ushenko, V. A., & Gavrylyak, M. S. (2013). Azimuthally invariant Mueller-matrix mapping of biological tissue in differential diagnosis of mechanisms protein molecules networks anisotropy. *Proc. SPIE 8812, Biosensing and Nanomedicine VI*, 88120Y.
3. Ushenko, V. A., & Gorsky, M. P. (2013). Complex degree of mutual anisotropy of linear birefringence and optical activity of biological tissues in diagnostics of prostate cancer. *Optics and Spectroscopy*, 115(2), 290–297.
4. Ushenko, Yu. A., Ushenko, V. A., Dubolazov, A. V., Balanetskaya, V. O., & Zabolotna, N. I. (2012). Mueller-matrix diagnostics of optical properties of polycrystalline networks of human blood plasma. *Optics and Spectroscopy*, 112(6), 884–892.
5. Ushenko, Yu. A., Dubolazov, A. V., Balanetskaya, V. O., Karachevtsev, A. O., & Ushenko, V. A. (2012). Wavelet-analysis of polarization maps of human blood plasma. *Optics and Spectroscopy*, 113(3), 332–343.
6. Ushenko, V. O. (2013). Spatial-frequency polarization phasometry of biological polycrystalline networks. *Optical Memory and Neural Networks*, 22(1), 56–64.

7. Ushenko, V. A., Pavlyukovich, N. D., & Trifonyuk, L. (2013). Spatial-Frequency Azimuthally Stable Cartography of Biological Polycrystalline Networks. *International Journal of Optics*, 7.

8. Ungurian, V. P., Ivashchuk, O. I., & Ushenko, V. O. (2011). Statistical analysis of polarizing maps of blood plasma laser images for the diagnostics of malignant formations. *Proc. SPIE 8338*, 83381L.

9. Ushenko, V. A., Dubolazov, O. V., & Karachevtsev, A. O. (2014). Two wavelength Mueller matrix reconstruction of blood plasma films polycrystalline structure in diagnostics of breast cancer. *Applied Optics*, 53(10), B128-B139.

10. Prysyazhnyuk, V. P., Ushenko, Yu. A., Dubolazov, A. V., Ushenko, A. G., & Ushenko, V. A. (2016). Polarization-dependent laser autofluorescence of the polycrystalline networks of blood plasma films in the task of liver pathology differentiation. *Appl. Opt.*, 55, B126-B132.

Метою роботи є узагальнення методів лазерної поляриметрії на випадок частково деполяризуючих оптично анізотропних полімерних шарів.

Ключові слова: поляризація; оптична анізотропія; метилакрилати; контроль температури.

Надійшла до редакції 12.05.22